

See discussions, stats, and author profiles for this publication at: <https://www.researchgate.net/publication/227777421>

Crystal structure of cyclophilin A complexed with a binding site peptide from the HIV-1 capsid protein

ARTICLE *in* PROTEIN SCIENCE · NOVEMBER 2008

Impact Factor: 2.85 · DOI: 10.1002/pro.5560061103

CITATIONS

56

READS

30

5 AUTHORS, INCLUDING:



Felix Vajdos

Pfizer Inc.

25 PUBLICATIONS 4,229 CITATIONS

[SEE PROFILE](#)

Crystal structure of cyclophilin A complexed with a binding site peptide from the HIV-1 capsid protein

FELIX F. VAJDOS, SANGHEE YOO, MEGAN HOUSEWEART,
WESLEY I. SUNDQUIST, AND CHRISTOPHER P. HILL

Department of Biochemistry, University of Utah, Salt Lake City, Utah 84132

(RECEIVED March 3, 1997; ACCEPTED July 11, 1997)

Abstract

The cellular protein, cyclophilin A (CypA), is incorporated into the virion of the type 1 human immunodeficiency virus (HIV-1) via a direct interaction with the capsid domain of the viral Gag polyprotein. We demonstrate that the capsid sequence $^{87}\text{His-Ala-Gly-Pro-Ile-Ala}^{92}$ ($^{87}\text{HAGPIA}^{92}$) encompasses the primary cyclophilin A binding site and present an X-ray crystal structure of the CypA/HAGPIA complex. In contrast to the *cis* prolines observed in all previously reported structures of CypA complexed with model peptides, the proline in this peptide, Pro 90, binds the cyclophilin A active site in a *trans* conformation. We also report the crystal structure of a complex between CypA and the hexapeptide HVGPIA, which also maintains the *trans* conformation. Comparison with the recently determined structures of CypA in complexes with larger fragments of the HIV-1 capsid protein demonstrates that CypA recognition of these hexapeptides involves contacts with peptide residues Ala(Val) 88, Gly 89, and Pro 90, and is independent of the context of longer sequences.

Keywords: cyclophilin A; HIV-1 capsid; pseudo-symmetry; X-ray crystallography

Like other retroviruses, formation of the human immunodeficiency virus type 1 (HIV-1) virion is driven by assembly of the Gag polyprotein. Gag binds to the inner leaflet of the host cell membrane and assembles into budding virions, each of which contain ~2,000 Gag molecules (Gelderblom et al., 1992; Hunter, 1994). Upon budding, Gag is cleaved by the viral protease to yield the individual Gag-derived proteins, which include matrix, capsid, and nucleocapsid. Following proteolysis, the capsid protein rearranges to form the cone-shaped core of the virion (a process termed maturation).

Approximately 200 copies of the abundant cytosolic protein cyclophilin A (CypA) are also packaged into each HIV-1 virion (Franke et al., 1994; Thali et al., 1994). Packaging of CypA results from a specific interaction with the capsid domain of Gag, and is essential for HIV-1 replication (Luban et al., 1993; Franke et al., 1994; Thali et al., 1994; Braaten et al., 1996a). In the absence of CypA, active viral reverse transcriptase is packaged at normal levels, and viral assembly, budding, and maturation all appear to proceed normally. However, replication of CypA-depleted virions is blocked at an early step in the HIV-1 life cycle following infection of a new cell. A leading hypothesis is that CypA assists in the disassembly of the capsid core (Braaten et al., 1996a; Gamble et al., 1996), although there is a report that the protein functions at

a later stage, following reverse transcription and preceding nuclear import (Steinkasserer et al., 1995).

Unlike HIV-1, the other primate lentiviruses (HIV-2 and SIV) do not package CypA (Braaten et al., 1996b). This property allowed others to use chimeric HIV-1/SIV viruses to map the CypA binding site to a 31 amino acid sequence in the amino terminal half of the HIV-1 capsid domain of Gag (Franke et al., 1994; Thali et al., 1994). A chimeric SIV virus encoding only 31 residues of the HIV-1 Gag capsid domain (residues 78–108)-packaged cyclophilin A. Conversely, a chimeric HIV-1 virus in which capsid residues 78–108 were replaced by the corresponding SIV capsid sequence did not package cyclophilin A. Directed mutagenesis further identified capsid residues Gly 89 and Pro 90 as critical for CypA binding (Franke & Luban, 1995; Braaten et al., 1996a; Yoo et al., 1997).

To define the interaction between HIV-1 capsid protein and CypA more precisely, we have used affinity chromatography to demonstrate that residues 87–92 of HIV-1 capsid ($^{87}\text{HAGPIA}^{92}$) form the primary CypA binding determinant. This hexapeptide sequence was therefore crystallized in complex with CypA and the structure determined. To examine the structural consequences of substitutions at position 88 (Ala 88), a variant of this hexapeptide (HVGPPIA) was also crystallized in complex with CypA and the structure determined. These experiments demonstrate that the HAGPIA hexapeptide functions as an autonomous CypA recognition element, and that CypA can accommodate larger side chains at position 88 with essentially no change in binding conformation.

Reprint requests to: Christopher P. Hill, Department of Biochemistry, University of Utah, Salt Lake City, Utah 84132; e-mail: chris@msscc.med.utah.edu.

Results

The HIV-1 capsid sequence $^{87}\text{HAGPIA}^{92}$ is the major determinant of cyclophilin A binding

A contiguous stretch of six capsid residues, $^{87}\text{His-Ala-Gly-Pro-Ile-Ala}^{92}$ (HAGPIA), is largely conserved in HIV-1 isolates that package and require CypA, but is highly variable in primate lentiviruses that do not package CypA (Franke et al., 1994; Braaten et al., 1996b). To test the hypothesis that this hexapeptide is the key determinant of CypA binding, we constructed and purified chimeric HIV-1/SIV capsid proteins containing: (1) the wild-type HIV-1_{NL4-3} sequence (CA1, positive control), (2) a chimeric capsid protein in which HIV-1 residues 78–108 were replaced by the corresponding SIV_{MAC239} sequence (CA2, negative control), and (3) a doubly chimeric capsid sequence in which the equivalent central SIV tetrapeptide (Pro-Ala-Pro-Glu) of CA2 was “restored” to the corresponding HIV-1 sequence $^{87}\text{HAGPIA}^{92}$ (CA3). As shown in Figure 1, native HIV-1 capsid protein (CA1) formed a specific complex with a purified glutathione-S-transferase-CypA fusion protein, whereas the chimeric CA2 capsid protein did not. The restored capsid protein, CA3, however, again bound to CypA, revealing that insertion of the HIV-1 hexapeptide $^{87}\text{HAGPIA}^{92}$ is sufficient to restore CypA binding in the context of a non-binding SIV capsid sequence. These experiments strongly implicate this hexapeptide as the primary binding determinant for CypA on the

HIV-1 capsid protein. This result is consistent with the previously reported structure of the CypA/CA_{1–151} complex, in which only residues 85–93 of CA_{1–151} interact with CypA (Gamble et al., 1996).

Crystal structure of the CypA/HAGPIA complex

To understand how CypA recognizes its capsid binding site, we determined the CypA/ $^{87}\text{HAGPIA}^{92}$ crystal structure. The space group of the crystals was P4₁ with six complexes in the asymmetric unit. The six complexes share nearly identical orientations, and are related to each other by non-crystallographic translations. This translational pseudo-symmetry closely approximates space group P4₃ with just one molecule in the asymmetric unit (Fig. 2A). This results in an unusual non-random distribution of intensities in the diffraction pattern, with the pseudo-lattice interspersed with two classes of reflection that we categorize as either weak or very weak (Fig. 2B). The one-sixth of the structure factor amplitudes that correspond to the pseudo-space group are on average 2.6 times larger than the remaining five-sixths of the data over the entire resolution range, with the difference in average intensity between the different classes of reflections (strong, weak, and very weak) decreasing at higher resolution (see Fig. 2C). Because of the difficulties inherent with refining crystal structures in the presence of pseudo symmetry, the initial structure determination and refinement were performed in the pseudo-space group.

Structure determination and refinement in the pseudo-space group

The structure was determined in the P4₃ pseudo-space group by molecular replacement using a 1.64 Å structure of CypA as the search model (Ke, 1993). The molecular replacement signal was unambiguous (correlation coefficient 0.49, $R = 44.3\%$ against all data from 15.0 to 3.0 Å; next highest solution CC = 0.17, $R = 55.0\%$) and the solution was further confirmed by simulated annealing omit maps (Brünger, 1992). The central four residues of the bound HAGPIA hexapeptide were clearly defined in unbiased electron density maps (Fig. 3). Although the N-terminal His has been modeled as a single conformer, poorly defined density may indicate the presence of two or more alternate conformations for this residue. Refinement against data from 15.0–1.58 Å reduced the R -factor to 34.3% (R -free 43.3%) with good stereochemistry; the correlation coefficient is 0.888 (free correlation coefficient 0.782). The R -factor against 15.0–2.5 Å data is 25.2% (R -free 37.4%). Despite numerous different refinement and rebuilding protocols the free R -factor failed to improve beyond this point. We attribute the limitations of this refinement to the approximations of the model that result from working in a pseudo-space group. The observation that average B factors are higher following refinement in the pseudo (P4₃; $\langle B \rangle = 27.2 \text{ \AA}^2$) compared to the true (P4₁; $\langle B \rangle = 16.6 \text{ \AA}^2$) space group (see below), suggests that differences between pseudo-symmetrically-related molecules are being modeled as thermal disorder in the pseudo-space group. Electron density is clearly defined for many residues, while in other areas, especially surface loops of CypA, the density is more diffuse. Although it is common for some surface loops to be poorly defined by X-ray crystallography, in this case the relatively large amount of poor quality density likely results from breakdown in the pseudo-symmetry.

The structure was further confirmed at 2.55 Å resolution by the method of multi-wavelength anomalous diffraction (MAD) from

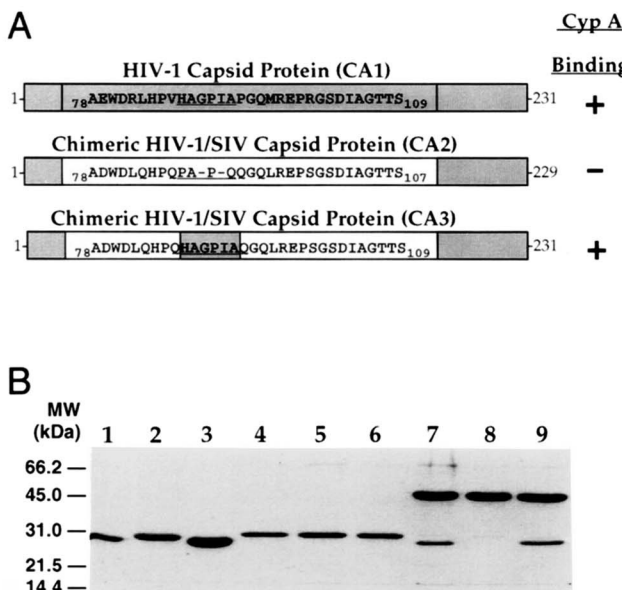
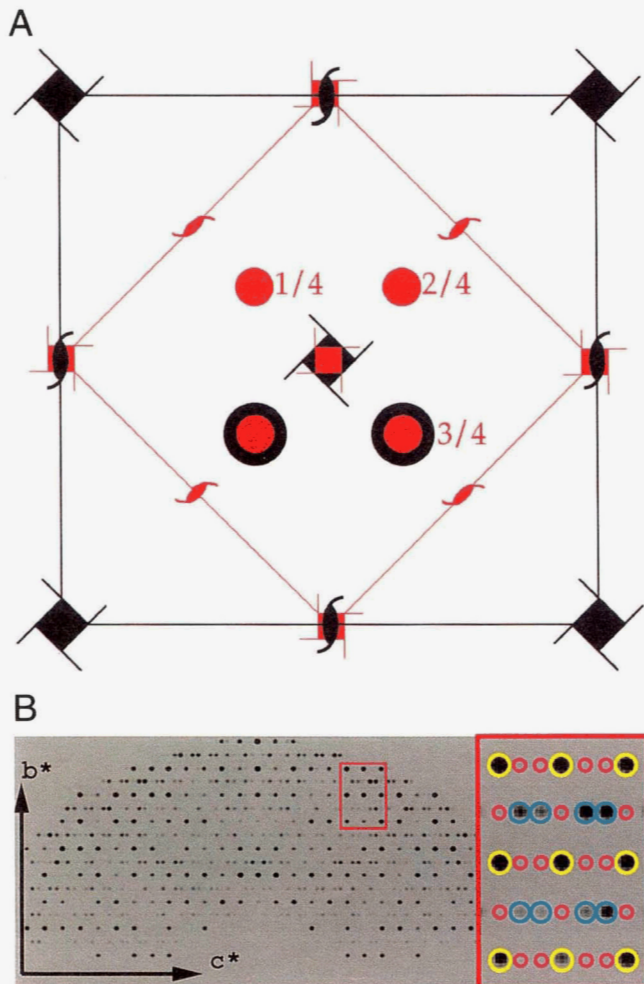


Fig. 1. **A:** Chimeric HIV-1/SIV capsid proteins used to identify the primary binding determinant for cyclophilin A on HIV-1 capsid are shown schematically. HIV-1_{NL4-3} sequences are shaded and SIV_{MAC239} sequences are shown in white. **B:** Glutathione-S-transferase (GST) or glutathione-S-transferase-cyclophilin A fusion protein (GST-CypA) were incubated with capsid proteins and GST or GST-CypA were subsequently removed from solution by incubation with glutathione Sepharose. Sepharose-bound proteins were visualized by SDS PAGE with Coomassie Blue staining. Lanes 1–3 (size controls). Lane 1, HIV-1 capsid (CA1) protein. Lane 2, CA2 protein. Lane 3, CA3 protein. Lanes 4–6 (negative controls). Lane 4, CA1 incubated with GST. Lane 5, CA2 incubated with GST. Lane 6, CA3 incubated with GST. Lane 7, CA1 incubated with GST-CypA. Lane 8, CA2 incubated with GST-CypA. Lane 9, CA3 incubated with GST-CypA. CA1 and CA3 proteins bind to CypA (arrow), whereas the CA2 protein does not.



selenomethionine-substituted protein (Hendrickson, 1991; Ramakrishnan & Biou, 1997). All four ordered methionine residues of CypA were substituted by selenomethionine and the experimental map was in good agreement with the solution obtained by molecular replacement.

Fig. 2. **A:** The a , b planes of the true $P4_1$ space group (black) and pseudo- $P4_3$ space group (red) are shown super-imposed. The perpendicular c axis is three times longer for the true ($P4_1$) compared to the pseudo ($P4_3$)-cell. The CypA/HAGPIA complexes stack in columns along the twofold screw axes of the pseudo- $P4_3$ space group, with the CypA active site and bound peptides at the interface between successive pseudo- 2_1 -related molecules in these columns. The relationship between the true $P4_1$ and the pseudo- $P4_3$ operator in the center of the figure is illustrated for an object represented as a black circle ($P4_1$) and a red dot ($P4_3$); three pseudo- $P4_3$ operations corresponds to one exact $P4_1$ operation. For the super-imposed pseudo- $P4_3$ and exact $P2_1$ operators at the corner of the pseudo-cell, six pseudo- $P4_3$ operations corresponds to one exact $P2_1$ operation. **B:** A pseudo-precession photograph illustrating the pseudo-symmetry in reciprocal space. These data were indexed and processed in the true $P4_1$ space group. The hemisphere shown is from the $0kl$ layer. Inset: The strong ($h + k = 2n, l = 3n$), weak ($h + k \neq 2n, l \neq 3n$), and pseudo-systematically absent ($h + k = 2n, l \neq 3n; h + k \neq 2n, l = 3n$) reflection classes are marked with yellow, cyan, and magenta circles, respectively. **C:** Mean structure factor amplitude as a function of $1/d^2$. Squares: strong, $\langle F/\sigma(F) \rangle = 33.3$. Diamonds: weak, $\langle F/\sigma(F) \rangle = 21.5$. Circles: pseudo-systematically absent, $\langle F/\sigma(F) \rangle = 7.0$.

Crystallographic analysis in the true space group

Refinement was continued in the true ($P4_1$) space group. All six molecules in the asymmetric unit were positioned by molecular replacement, and refined against 1.58 \AA data to an R -factor of

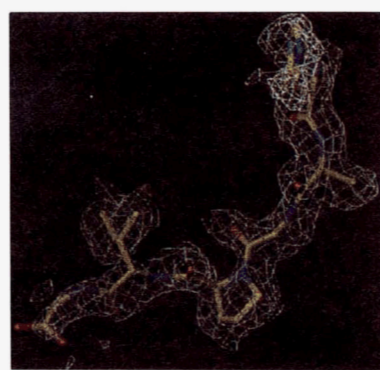
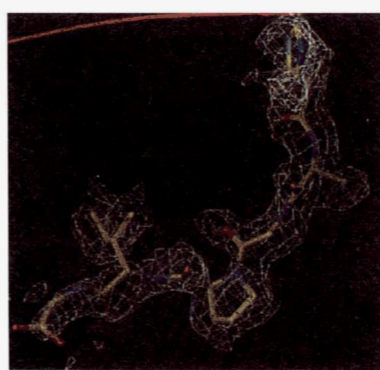


Fig. 3. The HAGPIA peptide conformation is defined in unbiased electron density. This $F_o - F_c$ map (6.0 to 2.5 \AA resolution, 1.3 RMSD) was computed in the pseudo ($P4_3$) cell using phases calculated from the refined molecular replacement model (no peptide or water molecules).

39.6% (*R*-free 46.1%) and correlation coefficient of 0.899 (free correlation coefficient 0.872). Although this high *R*-factor would typically indicate serious errors, high values are expected in the case of translational pseudo-symmetry, which causes a dramatic departure from the assumption of randomly distributed atoms that underlies usual interpretations of the *R*-factor (Wilson, 1950). Because the *R*-factor is a measure of the fractional agreement between observed and calculated structure factors, the high *R*-factor in this case can be attributed in large part to the abundance of weak data. After refinement against all data to 1.58 Å in the true space group, the *R*-factor against the subset of reflections that correspond to the pseudo P4₃ cell is 28.4% (*R*-free 33.1%). At 2.5 Å resolution, however, the *R*-factor against this subset of reflections is 21.6% and the free *R*-factor is 26.4%. Although this is an improvement over the values obtained from refinement in the pseudo-cell, it is still short of expectations for well-refined structures (a full evaluation of the crystallographic analysis is given in Materials and methods). Thus, despite high resolution data, refinement is limited by the preponderance of low intensity reflections.

Deviations from the pseudo-symmetry are best described as global rotations and translations of the CypA/HAGPIA complexes as rigid units (Fig. 4), with small differences in intermolecular contacts seen between the complexes. The differences in orientation between the six complexes range from 1° to 6°, and the deviations from crystallographic (P4₃) translations range from 0.1 Å to 6 Å in the *a* and *b* directions of the P4₁ unit cell. There are essentially no deviations from crystallographic (P4₃) translations in the *c* direction.

The six HAGPIA hexapeptides in the asymmetric unit show variable degrees of order. The C-terminal Ala lacks defined density in all six hexapeptides of the true space group. The N-terminal His is well defined in only one of the six complexes, and in two cases this residue completely lacks density. The central AGPI residues are clearly defined in all six complexes.

The 2.55 Å MAD map calculated in the true P4₁ space group confirmed the correctness of the structure determination (Fig. 5). The refinement was not obviously improved by inclusion of phase restraints at 2.55 Å resolution, however, and it was not possible to include phase restraints with the high resolution native data due to a lack of isomorphism between the native and selenomethionine-substituted crystals.

Description of the structure

Description of the structure will focus primarily on features that are apparent from crystallographic analysis in the pseudo-cell (Fig. 6). Cyclophilin A adopts the same eight-stranded anti-parallel β-barrel structure in the CypA/HAGPIA complex as seen in all other structure determinations (Kallen et al., 1991; Ke, 1992; Ke et al., 1993, 1994a; Pflügl et al., 1993; Thériault et al., 1993; Mikol et al., 1994; Zhao & Ke, 1996). There are no significant changes in CypA conformation upon binding HAGPIA, aside from minor rearrangement of Arg 55. Complex formation buries a total of 725 Å² of solvent accessible surface area (415 Å² on HAGPIA and 310 Å² on CypA) (Hubbard & Thornton, 1993). The peptide proline binds in the same hydrophobic pocket as proline residues of other CypA complexes. The peptide binds in an extended, crescent shape, with six direct hydrogen bonds to CypA active site residues and two water-mediated hydrogen bonding interactions (Fig. 6C). All of the hydrogen bonds between the hexapeptide and CypA are to main-chain atoms of the peptide ligand. Although a hydrogen

bond is reported between the peptide His ND1 and CypA Asn 71 O for CypA complexes with both CA_{1–151} (Gamble et al., 1996) and a 25-residue peptide of HIV-1 (residues 81 to 105; CA_{81–105}) (Zhao et al., 1997), this hydrogen bond is not seen in the CypA/HAGPIA structure, where the His residue is poorly ordered.

The peptide bond immediately prior to the hexapeptide Pro is in the *trans* conformation and the preceding Gly 89 adopts ϕ, ψ angles (both 141°) that are forbidden for residues other than glycine. Furthermore, the Gly89 CA atom is buried against CypA such that accommodation of a larger residue at this position would be excluded by steric hindrance. Thus, the CypA/HAGPIA complex is similar to both the CypA/CA_{1–151} (Gamble et al., 1996) and CypA/CA_{81–105} complexes (Zhao et al., 1997). Capsid residues 87–91 in the CypA/CA_{1–151} co-crystal structure super-impose upon the first five residues of the hexapeptide with a root-mean-square displacement (RMSD) of 0.5 Å for main chain atoms, and 0.9 Å for all atoms. When only the central Ala, Gly, and Pro residues of

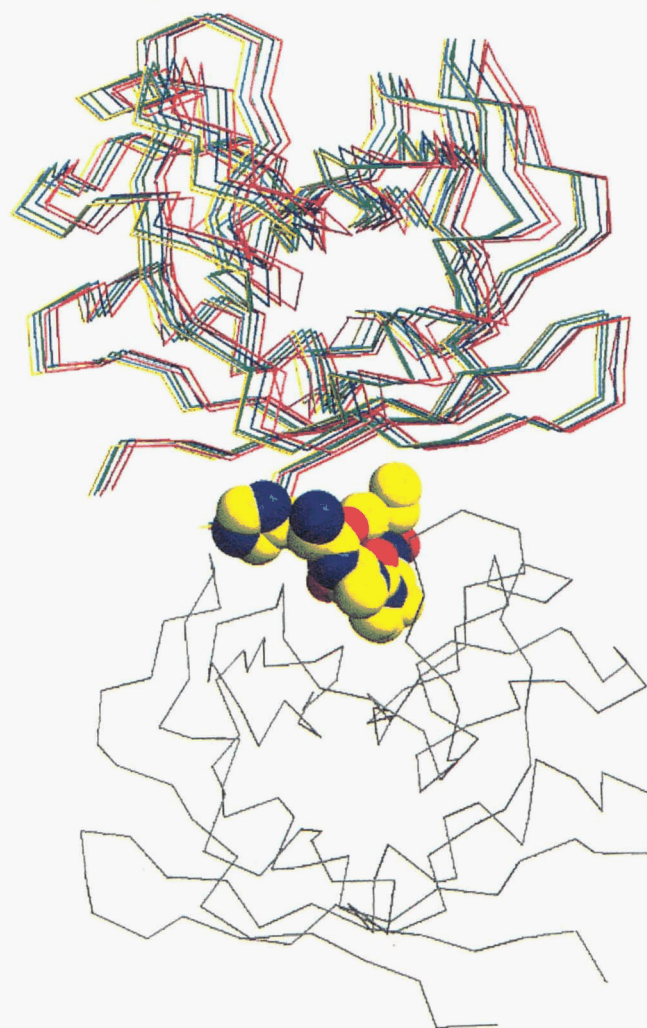


Fig. 4. Pseudo symmetrically related molecules differ by global rotations of 1° to 6° and shift of 0.1 Å to 6.3 Å in the *xy* plane. The six CypA/HAGPIA complexes in the asymmetric unit are shown superimposed in gray, with their bound HAGPIA peptide in CPK, and with their respective neighboring CypA molecules shown in different colors. If the pseudo-symmetry was exact crystallographic symmetry then the neighboring CypA molecules would superimpose with each other exactly.

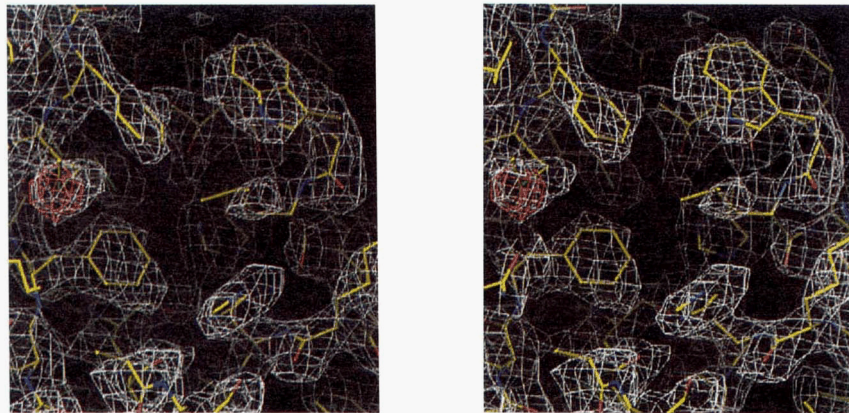


Fig. 5. The MAD/DM map, contoured in cyan at 0.9 RMSD, is calculated at 15–2.55 Å resolution in the true ($P4_1$) space group. The anomalous difference Fourier map is contoured in red at 6 RMSD.

the peptide are considered, the RMSD is 0.2 Å for all atoms, indicating that the binding geometry of this short stretch of residues by CypA is independent of the context of the rest of the capsid protein. This is consistent with the observations that residues 85–93 of CA_{1–151} lie in an exposed loop (Gamble et al., 1996; Gitti et al., 1996) and that the specificity determinant can be transferred from one lentiviral capsid protein to another. Tight binding, however, likely requires full length capsid to relieve the entropic cost of holding this sequence in a single conformation.

Crystal structure of the CypA/HVGPIA complex

In addition to Gly 89 and Pro 90, which are highly conserved in HIV-1, the side-chain of Ala 88 also contacts CypA in the co-crystal structures. However, HIV-1 isolates that package CypA have been identified in which this residue is replaced with the larger residues Val or Met (Braaten et al., 1996b). To understand how substitution for a larger residue can be accommodated in the CypA binding site, the crystal structure of CypA in complex with the hexapeptide HVGPIA was determined. CypA/HVGPIA crystals were approximately isomorphous to the parent HAGPIA peptide complex, and exhibit the same $P4_1$ ($P4_3$) pseudo-symmetry. Data were collected to 2.34 Å resolution and the peptide structure built into unbiased electron density maps. As for the parent complex, translational pseudo-symmetry precludes a robust atomic refinement. In the true $P4_1$ space group the *R*-factor is 35.8% (*R*-free 46.0%) and the correlation coefficient is 0.888 (free correlation coefficient 0.785), and in the pseudo- $P4_3$ cell the *R*-factor is 31.5% (*R*-free 35.1%) with a correlation coefficient of 0.85 (free correlation coefficient (0.81)). Despite the high *R*-factors, the peptide conformation is clearly defined in simulated annealing omit maps (Brünger, 1992).

The HVGPIA hexapeptide conformation and its interactions with CypA are very similar to those of the parent HAGPIA complex (Fig. 7). The Ala-Val substitution is accommodated by a small shift of the peptide backbone that is significant only for peptide residues His (0.6 Å), Val (0.5 Å), and Gly (0.3 Å), and is negligible for residues Pro, Ile, and Ala (<0.3 Å). Because of this small shift, the peptide valine CG1 and CG2 atoms maintain contacts to CypA that are chemically similar to those observed for the Ala 88 CB atom of the parent hexapeptide. In the CypA/HAGPIA structure, the

Ala 88 CB is in van der Waals contact (<4.1 Å) with CypA Asn 102 CA and C, and Ala 103 CB. In the CypA/HVGPIA complex the Val 88 CB atom does not contact CypA; rather, the Val 88 CG1 atom contacts Asn 102 CA and C, while the CG2 atom contacts CypA Ala 103 CB. The peptide valine CG1 atom participates in four additional van der Waals contacts with CypA Ala 101 CB and C, and with Gln 111 CB and CD. All other interactions between CypA and HVGPIA are maintained, and CypA active site residues are unchanged. Thus, Val, and perhaps larger residues, can be accommodated at this position with only minor backbone shifts of the peptide ligand while maintaining hydrophobic contacts with CypA.

Discussion

The normal cellular functions of cyclophilins are poorly understood (Stamnes et al., 1992). Cyclophilin A is well known as the intracellular receptor for the clinically important immunosuppressant cyclosporine A (CsA), a fungal cyclic undecapeptide that binds to the CypA active site (Pflügl et al., 1993; Thériault et al., 1993). Various other biological functions have been suggested for cyclophilins, including roles in signaling pathways (Xu et al., 1992; Bram & Crabtree, 1994; Duina et al., 1996; Freeman et al., 1996), cell surface recognition (Anderson et al., 1993), the heat-shock response (Sykes et al., 1993; Weisman et al., 1996), and protein folding (Schmid, 1993). Cyclophilins are prolyl *cis-trans* isomerasers that can accelerate the rate of folding for some proteins both in vitro (Freskgård et al., 1992; Lilie et al., 1993; Schmid, 1993) and in vivo (Matouschek et al., 1995; Rassow et al., 1995). Cyclophilins have been shown to play twin roles in re-folding experiments with carbonic anhydrase and with Fab domains, accelerating folding by *cis-trans* isomerization of prolyl peptide bonds and serving as molecular chaperones to prevent aggregation of early folding intermediates (Freskgård et al., 1992; Lilie et al., 1993). One of the best characterized physiological roles for a cyclophilin is for the *Drosophila* protein Nina A, which appears to act as a molecular chaperone by specifically binding and escorting the major rhodopsin, Rh1, through the secretory pathway (Colley, 1991; Baker et al., 1994).

The work presented here on hexapeptide complexes is consistent with our earlier rationalization for the dual CypA activities of

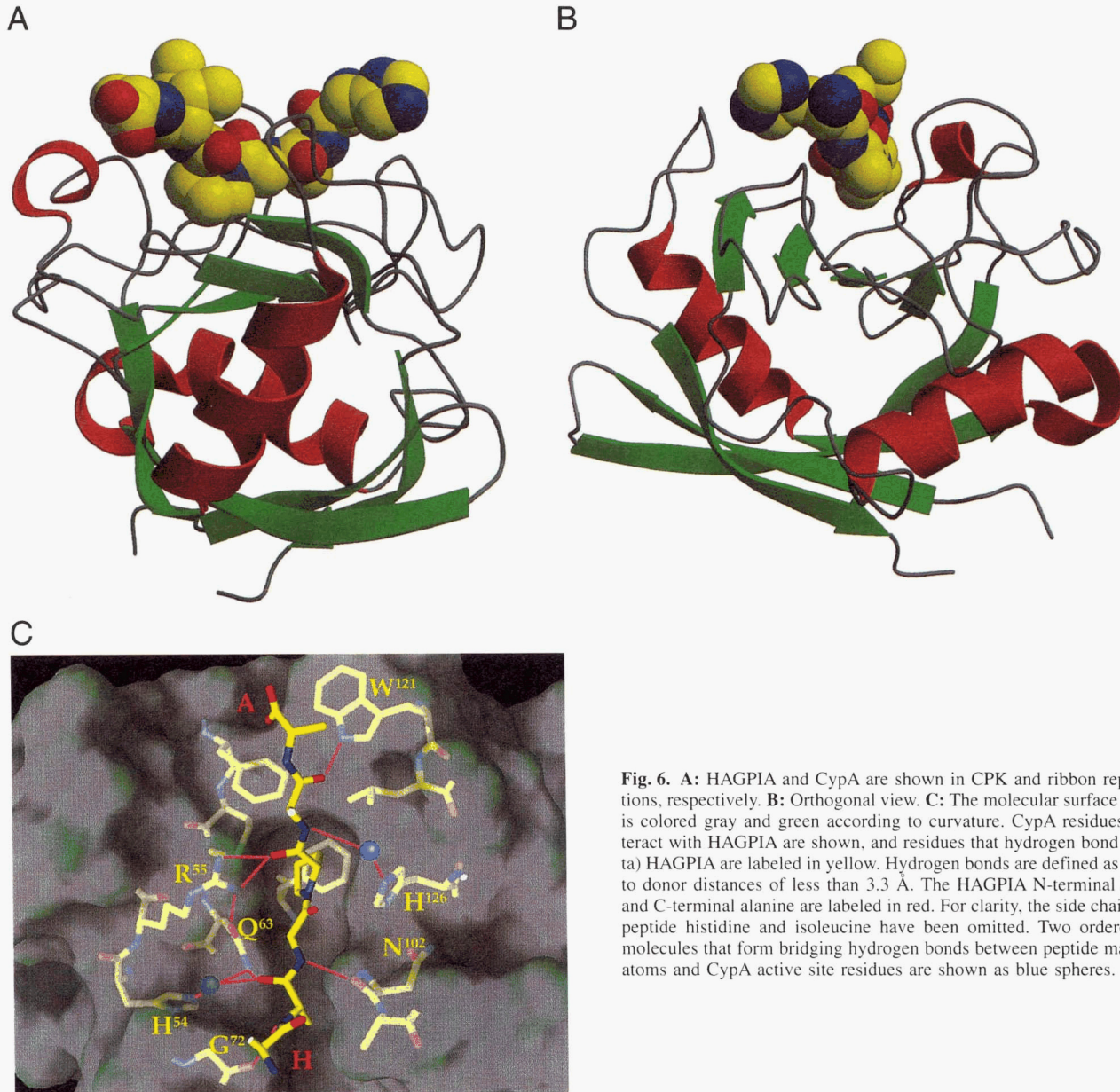


Fig. 6. **A:** HAGPIA and CypA are shown in CPK and ribbon representations, respectively. **B:** Orthogonal view. **C:** The molecular surface of CypA is colored gray and green according to curvature. CypA residues that interact with HAGPIA are shown, and residues that hydrogen bond (magenta) HAGPIA are labeled in yellow. Hydrogen bonds are defined as acceptor to donor distances of less than 3.3 Å. The HAGPIA N-terminal histidine and C-terminal alanine are labeled in red. For clarity, the side chains of the peptide histidine and isoleucine have been omitted. Two ordered water molecules that form bridging hydrogen bonds between peptide main chain atoms and CypA active site residues are shown as blue spheres.

specific binding and non-specific prolyl *cis-trans* isomerization (Gamble et al., 1996). We propose that specific binding is observed in some cases because the CypA active site is complementary to sequences containing the dipeptide Gly-*trans*-Pro. In contrast, binding of sub optimal binding sequences (i.e., X-Pro, X ≠ Gly) causes steric clash that is relieved in the *cis* conformation.

The side chain of the residue preceding Gly 89 in HIV-1 capsid also contributes to CypA binding. We have recently demonstrated that substitution of this residue, Ala 88, for Gly dramatically reduces binding affinity (44-fold), while substitution for the larger Val side chain is much less detrimental (3.4-fold) (Yoo et al., 1997). The CypA/HVGPIA structure shows how larger residues, such as Val, maintain equivalent interactions as for Ala 88, and thereby explains why this substitution causes only a modest reduction in the CypA/capsid binding affinity (Yoo et al., 1997). Presumably the large reduction in binding affinity upon substituting Ala 88

for Gly results from the loss of van der Waals interactions between the peptide Ala 88 CB methyl group and CypA.

The capsid proteins of HIV-2_{ROD} and SIV_{SM}PBJ do not appear to bind CypA, despite conservation of the Gly-Pro motif observed in HIV-1 (Braaten et al., 1996b). Instead of alanine or valine immediately N-terminal to Gly, the capsid proteins from these viruses contain a proline. Substitution of Ala 88 by proline, with its imide rather than amide nitrogen, would abolish the hydrogen bond observed between the Ala 88 amino group and the carbonyl oxygen of CypA Gly 72 (Fig. 6C). This H-bond is observed in the CypA/CA₁₋₁₅₁ structure (Gamble et al., 1996) as well as in both the CypA/HAGPIA and CypA/HVGPIA complexes, indicating that it is an important stabilizing interaction for the CypA/capsid complex. Furthermore, substitution of Ala 88 for Pro in the CypA/HAGPIA crystal structure would, assuming no conformational change to CypA or ligand, replace this favorable interaction with

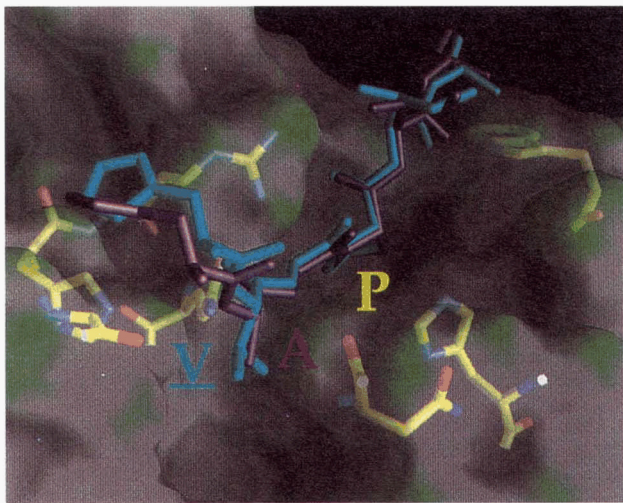


Fig. 7. Superposition of HAGPIA and HVGPIA peptides refined in the pseudo ($P4_3$)-cell. CypA CA atoms (residues 2–165) were overlapped by least squares (Kabsch, 1976). CypA residues that hydrogen bond the peptide ligands are shown. HAGPIA (magenta), HVGPIA (cyan). Ala/Val 88 and the peptide proline residues are labeled.

unacceptable steric clashes between the Gly 72 carbonyl oxygen and the proline CD (1.9 Å) and CG (2.6 Å) atoms.

The data presented here suggest that CypA can function as a sequence-specific binding protein, with a strong preference for the sequence X-Gly-*trans*-Pro (X ≠ Gly or Pro). This conclusion challenges the long-held assumption that CypA functions primarily as a non-specific proline isomerase. In analogy to NinaA, the normal *in vivo* function of CypA may be to act as a sequence specific protein chaperone, perhaps with specific substrates containing the X-Gly-*trans*-Pro (X ≠ Gly or Pro) motif on exposed surface loops, as seen in HIV-1 capsid. Given the high degree of sequence conservation among cyclophilins, especially of the residues which interact with both of the hexapeptides presented here (~90%) (Stamnes et al., 1992), it is possible that other cyclophilins also bind the Gly-*trans*-Pro dipeptide motif, perhaps modulating specificity by accommodating different flanking sequences as is seen at the Ala 88 position of HIV-1 capsid.

Materials and methods

Identification of the primary cyclophilin A binding site on HIV-1 capsid

The PstI-SpeI restriction fragment of the plasmid WISP93-73 (Yoo et al., 1997) was replaced with synthetic oligonucleotide sequences encoding either SIV capsid residues 78 to 107 or SIV capsid residues 78 to 86 and 91 to 107 interrupted by a sequence encoding HAGPIA. The HIV-1/SIV chimeric capsid proteins were purified in the same way as native HIV-1 capsid (Yoo et al., 1997). Glutathione-S-transferase (GST) and GST-CypA fusion protein were expressed in *E. coli* and purified by glutathione affinity chromatography followed by cation exchange chromatography. GST (50 μM) or GST-CypA (50 μM) were incubated with 50 μM purified capsid proteins for 30 min at 4°C in 20 mM Tris-HCl, 100 mM KCl, 2 mM CaCl₂, 2 mM MgCl₂, 5 mM DTT, 5% glycerol, 0.5% NP-40, pH 8.0 (Luban et al., 1993). GST or GST-

CypA were subsequently removed from solution by incubation with glutathione Sepharose 4B (Pharmacia). Sepharose-bound proteins were washed, dissociated by boiling in 2% SDS, and visualized by SDS PAGE with Coomassie Blue staining.

Crystallization

Recombinant human CypA was expressed and purified as described (Yoo et al., 1997). Selenomethionine-substituted CypA (Se-CypA) was produced by expressing the protein in the methionine auxotroph B834(DE3) grown in M9 minimal medium supplemented with 60 mg/L selenomethionine (Studier & Moffatt, 1986). Quantitative incorporation of selenomethionine was confirmed by electrospray mass spectrometry (calculated molecular mass: 18,247 Da; observed molecular mass: 18,245(±3) Da). The hexapeptides HAGPIA and HVGPIA were synthesized by solid phase synthesis, purified by reverse phase HPLC, and confirmed by electrospray mass spectrometry. The peptides were dissolved at 4°C in 50% methanol and these stock solutions were stored at -20°C.

CypA:peptide complexes were made at 4°C as follows. Equal volumes of 1.2 mM CypA (in 100 mM Tris-HCl, pH 8.2) and 84% saturated (NH₄)₂SO₄ were mixed to give a final concentration of 0.6 mM CypA. The small amount of precipitate that formed upon addition of (NH₄)₂SO₄ typically redissolved upon gentle mixing. The peptide was gently added immediately prior to use to a final concentration of 6 mM (10-fold excess over CypA) and mixed by swirling the pipette tip through the solution. Drops (5 μL) of the CypA:peptide complex solution were equilibrated at 21°C against 1 mL of well solution (44–54% saturated (NH₄)₂SO₄, 100 mM Tris-HCl, pH 8.2). Crystals typically grew within seven days, reaching maximum size within 2 weeks. The crystals grew as long tetragonal rods, with maximum dimensions of 1 mm in length and a square cross section of 0.1 mm on each edge.

X-ray data collection and processing

To overcome extreme radiation sensitivity at room temperature, all data were collected at 100 K. Crystals were transferred briefly (<15 s) to cryoprotectant solutions of either 20% polyethylene glycol 20 K, 8% butanediol, 100 mM (NH₄)₂SO₄, 50 mM Tris-HCl, pH 8.4 (CypA/HAGPIA and CypA/HVGPIA), or 65% saturated (NH₄)₂SO₄, 15% glycerol, 50 mM Tris-HCl, pH 8.2 (SeCypA/HAGPIA). Crystals were suspended in a small loop and cooled by plunging into liquid nitrogen. Data were collected on MAR imaging plate detectors at beamline X12C of the National Synchrotron Light Source (CypA/HAGPIA and SeCypA/HAGPIA), and at beamline 7-1 of the Stanford Synchrotron Radiation Laboratory (CypA/HVGPIA). Most calculations used programs from the CCP4 suite (CCP4, 1994). Data were processed and scaled using DENZO and SCALEPACK (Otwinowski, 1993). Data statistics are reported in Table 1.

Molecular replacement

The structure was determined by molecular replacement using the program AMoRe (Navaza, 1994) and a 1.64 Å structure of CypA as the search model (Ke et al., 1993) (PDB code 2cyh). The CypA search model used the protein alone (i.e., without the ordered water molecules or the bound Ala-Pro dipeptide of this complex structure). Using data from 15.0–3.0 Å, rigid body refinement gave *R*-factors of 47.0% in the true space group and 36.5% in the pseudo space group.

Table 1. Data statistics

	CypA/HAGPIA		SeCypA/HAGPIA		CypA/HVGPIA	
Resolution ^a (Å)	15–1.58		15–2.55		15–2.34	
High resolution (Å)	1.61–1.58		2.59–2.55		2.38–2.34	
Space group	P4 ₁	P4 ₃	P4 ₁	P4 ₃	P4 ₁	P4 ₃
Unit cell (Å)	<i>a</i> = <i>b</i> = 72.9 <i>c</i> = 188.5	<i>a</i> = <i>b</i> = 51.5 <i>c</i> = 62.8	<i>a</i> = <i>b</i> = 73.4 <i>c</i> = 190.2	<i>a</i> = <i>b</i> = 51.9 <i>c</i> = 63.4	<i>a</i> = <i>b</i> = 74.0 <i>c</i> = 190.4	<i>a</i> = <i>b</i> = 52.4 <i>c</i> = 63.4
#Obs.	1,295,142	214,067	159,378	26,762	284,842	48,608
#Unique ref.	147,562	24,895	32,487	5,576	42,633	7,251
Complete (%)	88.4 (54.8)	88.1 (51.9)	97.2 (98.0)	97.6 (95.7)	97.7 (80.1)	97.9 (78.6)
<i>R</i> _{sym} (<i>I</i>) ^b (%)	8.8 (27.8)	8.6 (15.6)	7.5 (20.6)	3.5 (7.9)	11.0 (29.4)	4.7 (11.4)
(<i>I</i> / σ <i>I</i>)	4.2	9.4	6.0	19.1	4.7	17.6
(2 σ) (%)	29.3 (44.5)	10.7 (30.2)	51.3 (62.2)	9.2 (19.7)	50.2 (48.6)	9.8 (20.3)

^aThe data for CypA/HAGPIA extend to 1.53 Å resolution. However, because of detector geometry the completeness beyond 1.58 Å is less than 50%. Thus, the resolution of this data set is reported as 1.58 Å. All intercepted data are considered observed, with no application of a sigma cut. All data from 15.0 Å to 1.53 Å were used in the refinement. Numbers in parentheses refer to the high resolution shell.

$$R_{\text{sym}}(I) = 100 * \sum_{hkl} \sum_i |I_i - \langle I \rangle| / \sum \langle I \rangle$$

MAD phase determination

Data from a SeCypA/HAGPIA complex crystal were collected at three wavelengths: λ1 (0.9794 Å, minimum *f'*), λ2 (0.9788 Å, maximum *f''*), and λ3 (0.9300 Å, maximum *f'*). These three data sets were processed separately, and scaled to each other with SCALEIT (CCP4, 1994).

The “anomalous” (λ2) and “isomorphous” (λ3-λ1) difference Patterson functions display strong peaks that are identical to those expected from the molecular replacement solution. An “anomalous” difference Fourier, computed with model phases –90°, showed high peaks ($>10 \times$ RMSD) for all the Met SD atoms. Selenium refinement and phase calculation with MLPHARE (Otwinowski, 1991) was followed by solvent leveling and histogram shifting with DM (Cowtan, 1994).

Refinement

Numerous refinement protocols were investigated using the program XPLOR (Engh & Huber, 1991; Brünger, 1996), including rigid body, simulated annealing molecular dynamics, torsion angle dynamics, positional, and overall, grouped and atomic *B* factor. The success of refinement was monitored by the *R*-free (Brünger, 1992) and from the appearance of unbiased electron density, such as that for the peptide before its inclusion in the model and for simulated annealing omit maps. Approaches investigated included starting refinement from a subset of the available data (medium resolution or strong data), and gradually adding more terms, with either increasing resolution or decreasing amplitude. Refinement cycles were interspersed with manual rebuilding (Jones et al., 1991). The most successful approach started by refining in the pseudo (P4₃)-cell, followed by expansion to the true (P4₁) cell. Individual *B*-factor refinement performed better than grouped *B*-factor refinement, especially when the high resolution data were used. The best refinement used all data from 15.0 Å to the high resolution limit, including the very weak terms, with application of a bulk solvent correction (Jiang & Brünger, 1994). Simulated annealing omit maps were used to determine the most well-ordered residues of CypA, and tight non-crystallographic symmetry restraints applied to these residues in each of the six complexes in the asymmetric unit. Refinement statistics are reported in Table 2.

The refined model has good stereochemistry (Table 2) (Laskowski et al., 1993). Of 135 non-glycine, non-proline residues in the CypA/HAGPIA structure refined in the pseudo (P4₃)-space group, 98 are in the most favored regions of the Ramachandran plot, 36 are in additional allowed regions, and 1 is in a generously allowed region. No residues have disallowed ϕ , ψ angles. The PDB ID codes for the CypA/HAGPIA, SeCypA/HAGPIA, and CypA/HVGPIA complexes in the pseudo (P4₃)-space group are 1awq, 1aws, and 1awu, respectively, while in the true (P4₁) space group they are 1awr, 1awt, and 1awv, respectively.

Evaluation of the crystallographic analysis

Despite extensive effort at refinement, the crystallographic *R*-factors for these crystal structures fall short of those expected for data of this quality. The poor refinement in the pseudo-P4₃ unit cell results from the breakdown in the symmetry relating adjacent molecules, while the poor refinement in the true P4₁ lattice stems largely from the preponderance of very weak data. Because the low amplitude terms have the effect of decreasing the value of the denominator in the crystallographic *R*-factor, systematically weak reflections will always result in a high *R* factor. In addition, small amplitudes inherently have a lower signal-to-noise ratio, thereby limiting the ability to distinguish genuine differences between molecules from random experimental noise. Thus, the structures we report here are less precisely determined than more normally distributed structures of comparable quality.

Because of the unusual pseudo-symmetry of these crystals, we have considered other possible explanations for the observed diffraction distribution. The possibility of merohedrous twinning, in which both lattices superimpose exactly, has been evaluated from the distribution function *N*(*Z*, α) versus *Z* (Rees, 1980). When considering all data, or various subgroups such as the strong “P4₃,” or pseudo-systematically weak terms, the predicted twinning fraction was always zero (Kleywegt & Jones, 1994). We also note that data have now been collected from three crystals, and in every case the ratio of structure factor amplitudes for the three classes of reflections shown in Figure 2D is always 1.0/0.54/0.11 (strong/weak/pseudo-absent) over the resolution range 15–2.55 Å. Thus, any twinning effect must always occur with the same twinning fraction.

Table 2. Refinement statistics

	CypA/HAGPIA		SeCypA/HAGPIA		CypA/HVGPIA	
Space group	P4 ₁	P4 ₃	P4 ₁	P4 ₃	P4 ₁	P4 ₃
R-factor ^a (%)	39.4 (48.1)	34.3 (47.8)	37.8 (42.2)	26.2 (40.3)	35.8 (40.4)	31.5 (40.2)
R-free ^b (%)	46.1 (49.5)	43.3 (39.4)	46.5 (46.3)	33.7 (62.6)	46.0 (49.1)	35.1 (50.0)
CC ^c	0.87	0.89	0.88	0.88	0.89	0.85
CC-free	0.82	0.78	0.78	0.80	0.78	0.81
# Residues	1,020	170	1,020	170	1,020	170
# Waters	175	52	175	52	175	13
$\langle B \rangle$ (Å ²)						
CypA	16.6	27.4	16.6	26.6	16.6	27.8
Peptide	15.9	17.8	15.9	16.9	15.9	22.0
Water	15.0	30.5	15.0	31.3	15.0	25.3
RMSD						
Bond(Å)	0.013	0.008	0.011	0.009	0.010	0.010
Angle (°)	1.611	1.410	1.500	1.476	1.455	1.592

^aR-factor = $100 * \sum(|F_P(obs)| - |F_P(calc)|) / \sum |F_P(obs)|$. The numbers in parentheses refer to the high resolution data shell (see Table 1).

^bR-free is the R-factor for a randomly selected subset (5%) of the data that have not been used for minimization of the crystallographic residual.

^cCC = linear correlation coefficient = $\langle f_{obs}f_{calc} - \langle f_{obs}\rangle\langle f_{calc}\rangle \rangle / (\langle f_{obs}^2 \rangle - \langle f_{obs}\rangle^2)(\langle f_{calc}^2 \rangle - \langle f_{calc}\rangle^2)^{1/2}$.

Pseudo-merohedrous twinning (i.e., two or more lattices overlap approximately, but not exactly, in three dimensions) is unlikely because all of the data observed in these crystals can be indexed to a single lattice relatively easily, with average chi-squared values of 1.0–2.5 using a standard positional error model of 0.05 mm in both the *x* and *y* dimensions of the scanner surface (Otwinowski, 1993). Thus, two independent lattices would have to be very closely aligned. Furthermore, the spot shape is very good for all classes of reflections in these data, with no indication of doublets.

The success in indexing all observed reflections to the P4₁ cell means that it is highly unlikely that different reflection classes originate from two or more separate lattices. It is possible, in principle, that indexing of all data to a single lattice might be an artifact, with small differences between two or more closely aligned lattices being lost in the frame by frame refinement of parameters such as unit cell dimensions, misalignment angles, and crystal to detector distance. This seems unlikely, however, because these

parameters do not vary significantly between frames. Furthermore, native Patterson maps calculated with data from the three reflection classes (strong, weak, and pseudo-systematically absent) show the same five pseudo origin peaks [(*u,v,w*) = (0,0,1/3), (0,0,2/3), (1/2,1/2,0), (1/2,1/2,1/3), and (1/2,1/2,2/3)], consistent with the view that the three groups of reflections arise from a single, crystallographic lattice.

We have also considered the possibility that the true space group is P4₃ with one complex per asymmetric unit (i.e., our pseudo-P4₃ cell), with random dislocations between layers of complexes, resulting in “off-lattice” reflections. Such random dislocations have been observed in crystals of inorganic salts or small organic molecules (Zachariassen, 1947, 1948; Paterson, 1952; Christian, 1954), and at least once in the case of protein crystals (Bragg & Howells, 1954; Cochran & Howells, 1954; Howells & Perutz, 1954). However, in the descriptions of diffraction from crystals exhibiting planar disorder, the disorder usually results in line-broadening or

Table 3. R factor versus data from different parity groups

Parity group	CypA/HAGPIA ^a R factor/R free		SeCypA/HAGPIA ^b R factor/R free		CypA/HVGPIA ^c R factor/R free	
	P4 ₁	P4 ₃	P4 ₁	P4 ₃	P4 ₁	P4 ₃
<i>h</i> + <i>k</i> = 2 <i>n</i> , <i>l</i> = 3 <i>n</i>	28.2/33.1 (21.6/26.4) ^d	34.3/43.3 (25.2/37.4)	22.9/29.9	26.1/33.7	23.5/31.7 (22.4/30.7)	31.5/35.1 (30.4/33.8)
<i>h</i> + <i>k</i> ≠ 2 <i>n</i> , <i>l</i> ≠ 3 <i>n</i>	42.5/50.8 (39.4/49.4)	—	41.5/53.0	—	39.4/51.2 (39.0/51.8)	—
<i>h</i> + <i>k</i> = 2 <i>n</i> , <i>l</i> ≠ 3 <i>n</i> or <i>h</i> + <i>k</i> ≠ 2 <i>n</i> , <i>l</i> = 3 <i>n</i>	47.9/52.5 (48.7/54.9)	—	56.5/59.7	—	50.1/56.2 (50.1/57.1)	—

^aR factor/R free reported for the resolution range 15.0–1.58 Å.

^bResolution range 15.0–2.55 Å.

^cResolution range 15.0–2.34 Å.

^dNumbers in parentheses are the R factor/R free over the resolution range 15.0–2.50 Å.

diffuse scattering, although in one case (Zachariasen, 1948), the diffuse reflections were seen to become sharp upon heat treatment of the crystals. The weak reflections observed in the present case are discrete reflections, and the mosaicity for the data processed as P4₁ (0.46°) is essentially that of the data processed as pseudo-P4₃ (0.42°). The weak and pseudo-absent reflections are not noticeably broader or more diffuse than the strong reflections in this lattice, and therefore are unlikely to be due to random dislocations within a P4₃ lattice.

We conclude, therefore, that our description of P4₁/P4₃ pseudo-symmetry represents the most likely arrangement of this crystal form. Similar pseudo-crystallographic translations have been observed in other protein crystals, notably cyclophilin C complexed with cyclosporin A (Ke et al., 1994b), and the enzyme chorismate mutase (Chook et al., 1993). The following points support our crystallographic analysis. First, the MAD map determined at 2.55 Å resolution from selenomethionine-substituted crystals is of high quality (Fig. 5). Second, unbiased omit maps, such as those obtained after simulated annealing refinement of a partial model, are well-defined (Fig. 3). Third, the structure seen for the bound peptide is essentially identical to that observed in two other independent studies (Gamble et al., 1996; Zhao et al., 1997). Fourth, although the R-factor is high for 1.58 Å data, the R-factors are quite reasonable at medium resolution against data for the pseudo-cell (Table 3). Finally, the free R-factor for the P4₃ (pseudo) space group data is improved when the pseudo-absent data from the P4₁ (true) space group are included in the refinement (Table 3). This indicates that both classes of reflections originate from the same crystal lattice, and is consistent with our understanding of the pseudo symmetry.

Acknowledgments

We thank Robert Sweet, Harmut Luecke, and Mike Soltis for assistance with data collection, Venki Ramakrishnan and members of the Hill and Sundquist laboratories for critical comments on the manuscript, and Hengming Ke for a preprint. This work was supported by grants from the National Institutes of Health (AI40333 to C.P.H. and W.I.S.), the Lucile P. Markey Foundation, and the University of Utah Research Committee. C.P.H. is the recipient of an American Cancer Society Junior Faculty Research Award. The University of Utah peptide synthesis core facility is supported by a grant from the National Cancer Institute (CA42014 to Robert Schackmann).

References

- Anderson SK, Gallinger S, Roder J, Frey J, Young HA, Ortaldo JR. 1993. A cyclophilin-related protein involved in the function of natural killer cells. *Proc Natl Acad Sci USA* 90:542–546.
- Baker EK, Colley NJ, Zuker CS. 1994. The cyclophilin homolog NinaA functions as a chaperone, forming a stable complex *in vivo* with its protein target rhodopsin. *EMBO J* 13:4886–4895.
- Braaten D, Franke EK, Luban J. 1996a. Cyclophilin A is required for an early step in the life cycle of human immunodeficiency virus type 1 before the initiation of reverse transcription. *J Virol* 70:3551–3560.
- Braaten D, Franke EK, Luban J. 1996b. Cyclophilin A is required for the replication of group M human immunodeficiency virus type 1 (HIV-1) and simian immunodeficiency virus SIV_{CPZ}GAB but not group O HIV-1 or other primate immunodeficiency viruses. *J Virol* 70:4220–4227.
- Bragg WL, Howells ER. 1954. X-ray diffraction by imidazole methaemoglobin. *Acta Crystallogr* 7:409–411.
- Bram RJ, Crabtree GR. 1994. Calcium signalling in T cells stimulated by a cyclophilin B-binding protein. *Nature* 371:355–358.
- Brünger AT. 1992. Free R value: A novel statistical quantity for assessing the accuracy of crystal structures. *Nature* 355:472–475.
- Brünger AT. 1996. *X-PLOR version 3.843, a system for X-ray crystallography and NMR*. New Haven, CT: Yale University.
- CCP4. 1994. The CCP4 suite: programs for protein crystallography. *Acta Crystallogr D* 50:760–763.
- Chook Y, Ke H, Lipscomb WN. 1993. Crystal structures of the monofunctional chorismate mutase from *Bacillus subtilis* and its complex with a transition state analog. *Proc Natl Acad Sci USA* 90:8600–8603.
- Christian JW. 1954. A note on deformation stacking faults in hexagonal close-packed lattices. *Acta Crystallogr* 7:415–416.
- Cochran W, Howells ER. 1954. X-ray diffraction by a layer structure containing random displacements. *Acta Crystallogr* 7:412–415.
- Colley NJ, Baker EK, Starnes MA, Zuker CS. 1991. The cyclophilin homolog NinaA is required in the secretory pathway. *Cell* 67:255–263.
- Cowtan KD. 1994. 'dm': An automated procedure for phase improvement by density modification. *Joint CCP4 and ESF-EACBM Newslett Protein Crystallogr* 31:34–38.
- Duina AA, Chang H-CJ, Marsh JA, Lindquist S, Gaber RF. 1996. A cyclophilin function in hsp90-dependent signal transduction. *Science* 274:1713–1715.
- Engh RA, Huber R. 1991. Accurate bond and angle parameters for X-ray protein structure refinement. *Acta Crystallogr A* 47:392–400.
- Franke EK, Luban J. 1995. Cyclophilin and gag in HIV-1 replication and pathogenesis. In: Andreu J-M, Lu W, eds. *Cell activation and apoptosis in HIV infection*. New York: Plenum Press. pp 217–228.
- Franke EK, Yuan HEH, Luban J. 1994. Specific incorporation of cyclophilin A into HIV-1 virions. *Nature* 372:359–362.
- Freeman BC, Toft DO, Morimoto RI. 1996. Molecular chaperone machines: Chaperone activities of the cyclophilin cyp-40 and the steroid aporeceptor-associated protein p23. *Science* 274:1718–1720.
- Freskgård P-O, Bergenhem N, Jonsson B-H, Svensson M, Carlsson U. 1992. Isomerase and chaperone activity of prolyl isomerase in the folding of carbonic anhydrase. *Science* 258:466–468.
- Gamble TR, Vajdos F, Yoo S, Worthylake DK, Housewright M, Sundquist WI, Hill CP. 1996. Crystal structure of human cyclophilin A bound to the amino-terminal domain of HIV-1 capsid. *Cell* 87:1285–1294.
- Gelderblom HR, Bauer PG, Özcel M, Höglund S, Niedrig M, Renz H, Morath B, Lundquist P, Nilsson Å, Mattow J, Grund C, Pauli G. 1992. Morphogenesis and morphology of human immunodeficiency virus. In: Aloia RC, Curtin CC, eds. *Membrane interactions of HIV*. New York: Wiley-Liss. pp 33–54.
- Gitti RK, Lee BM, Walker J, Summers MF, Yoo S, Sundquist WI. 1996. Structure of the amino-terminal core domain of the HIV-1 capsid protein. *Science* 273:231–235.
- Hendrickson WA. 1991. Determination of macromolecular structures from anomalous diffraction of synchrotron radiation. *Science* 254:51–58.
- Howells ER, Perutz MF. 1954. The structure of haemoglobin V. Imidazolemethaemoglobin: A further check of the signs. *Proc R Soc Lond A* 225:308–314.
- Hubbard SJ, Thornton JM. 1993. 'NACCESS', Computer Program, Department of Biochemistry & Molecular Biology, University College London.
- Hunter E. 1994. Macromolecular interactions in the assembly of HIV and other retroviruses. *Semin Virol* 5:71–83.
- Jiang JS, Brünger AT. 1994. Protein hydration observed by x-ray diffraction: Solvation properties of penicillopepsin and neuraminidase crystal structures. *J Mol Biol* 243:100–115.
- Jones TA, Zou J-Y, Cowan SW, Kjeldgaard M. 1991. Improved methods for building protein models in electron density maps and location of errors in these models. *Acta Crystallogr A* 47:110–119.
- Kallen J, Spitzfaden C, Zurini MGM, Wider G, Widmer H, Wüthrich K, Walkinshaw MD. 1991. Structure of human cyclophilin and its binding site for cyclosporin A determined by X-ray crystallography and NMR spectroscopy. *Nature* 353:276–279.
- Ke H. 1992. Similarities and differences between human cyclophilin A and other β-barrel structures. Structural refinement at 1.63 Å resolution. *J Mol Biol* 228:539–550.
- Ke H, Mayrose D, Cao W. 1993. Crystal structure of cyclophilin A complexed with substrate Ala-Pro suggests a solvent-assisted mechanism of *cis-trans* isomerization. *Proc Natl Acad Sci USA* 90:3324–3328.
- Ke H, Mayrose D, Belshaw PJ, Alberg DG, Schreiber SL, Chang ZY, Etzkorn FA, Ho S, Walsh CT. 1994a. Crystal structure of cyclophilin A complexed with cyclosporin A and N-methyl-4-[(E)-2-but enyl]-4,4-dimethylthreonine cyclosporin A. *Structure* 2:33–44.
- Ke H, Zhao Y, Luo F, Weissman I, Friedman J. 1994b. Crystal structure of murine cyclophilin C complexed with immunosuppressive drug cyclosporin A. *Proc Natl Acad Sci USA* 90:11850–11854.
- Kleywegt GJ, Jones TA. 1994. 'MOLEMAN' Computer Program, Department of Molecular Biology, Uppsala University.
- Laskowski RA, MacArthur MW, Moss DS, Thornton JM. 1993. PROCHECK: A program to check the stereochemical quality of protein structures. *J Appl Crystallogr* 26:283–291.
- Lilie H, Lang K, Rudolph R, Buchner J. 1993. Prolyl isomerases catalyze antibody folding *in vitro*. *Protein Sci* 2:1490–1496.

- Luban J, Bossolt KL, Franke EK, Kalpana GV, Goff SP. 1993. Human immunodeficiency virus type 1 gag protein binds to cyclophilins A and B. *Cell* 73:1067–1078.
- Matouschek A, Rospert S, Schmid K, Glick BS, Schatz G. 1995. Cyclophilin catalyzes protein folding in yeast mitochondria. *Proc Natl Acad Sci USA* 92:6319–6323.
- Mikol V, Kallen J, Walkinshaw MD. 1994. The X-ray structure of (MeBm_2O)¹⁻-cyclosporin complexed with cyclophilin A provides an explanation for its anomalously high immunosuppressive activity. *Prot Eng* 7:597–603.
- Navaza J. 1994. AMoRe: An automated package for molecular replacement. *Acta Crystallogr A* 50:157–163.
- Otwinowski Z. 1991. Maximum likelihood refinement of heavy atom parameters. In: Wolf W, Evans PR, Leslie AGW, eds. *Isomorphous replacement and anomalous scattering*. Warrington WA4 4AD, England: Daresbury Laboratory. pp 80–86.
- Otwinowski Z. 1993. Oscillation data reduction program. In: Sawyer L, Isaacs N, Bailey S, eds. *Data collection and processing*. Warrington WA4 4AD, England: SERC Daresbury Laboratory. pp 56–62.
- Paterson MS. 1952. X-ray diffraction by face-centered cubic crystals with deformation faults. *J Appl Phys* 23:805–811.
- Pflügl G, Kallen J, Schirmer T, Janssonius JN, Zurini MGM, Walkinshaw MD. 1993. X-ray structure of a decameric cyclophilin–cyclosporin crystal complex. *Nature* 361:91–94.
- Ramakrishnan V, Biou V. 1997. Treatment of multiwavelength anomalous diffraction as a special case of multiple isomorphous replacement. *Methods Enzymol* 276:538–557.
- Rassow J, Mohrs K, Koidl S, Barthelmeß IB, Pfanner N, Tropschug M. 1995. Cyclophilin 20 is involved in mitochondrial protein folding in cooperation with molecular chaperones Hsp70 and Hsp60. *Mol Cell Biol* 15:2654–2662.
- Rees DC. 1980. The influence of twinning by merohedry on intensity statistics. *Acta Crystallogr A* 36:578–581.
- Schmid FX. 1993. Prolyl isomerase: Enzymatic catalysis of slow protein-folding reactions. *Annu Rev Biophys Biomol Struct* 22:123–143.
- Stamnes MA, Rutherford SL, Zuker CS. 1992. Cyclophilins: A new family of proteins involved in intracellular folding. *Trend Cell Biol* 2:272–276.
- Steinkasserer A, Harrison R, Billich A, Hammerschmid F, Werner G, Wolff B, Peichl P, Palfi G, Schnitzel W, Mlynar E, Rosenwirth B. 1995. Mode of action of SDZ NIM 811, a nonimmunosuppressive cyclosporin A analog with activity against human immunodeficiency virus type 1 (HIV-1): Interference with early and late events in HIV-1 replication. *J Virol* 69:814–824.
- Studier FW, Moffatt BA. 1986. Use of bacteriophage T7 RNA polymerase to direct selective high-level expression of cloned genes. *J Mol Biol* 189:113–130.
- Sykes K, Gething M-J, Sambrook J. 1993. Proline isomerases function during heat shock. *Proc Natl Acad Sci USA* 90:5853–5857.
- Thali M, Bukovsky A, Kondo E, Rosenwirth B, Walsh CT, Sodroski J, Götzlinger HG. 1994. Functional association of cyclophilin A with HIV-1 virions. *Nature* 372:363–365.
- Thériault Y, Logan TM, Meadows R, Yu L, Olejniczak ET, Holzman TF, Simmer RL, Fesik SW. 1993. Solution structure of the cyclosporin A/cyclophilin complex by NMR. *Nature* 361:88–91.
- Weisman R, Creanor J, Fantes P. 1996. A multicopy suppressor of a cell cycle defect in *S. pombe* encodes a heat-shock inducible 40 kDa cyclophilin-like protein. *EMBO J* 15:447–456.
- Wilson AJC. 1950. Largest likely values for the reliability index. *Acta Crystallogr* 3:397–398.
- Xu Q, Leiva MC, Fischkoff SA, Handschumacher RE, Lytle CR. 1992. Leukocyte chemotactic activity of cyclophilin. *J Biol Chem* 267:11968–11971.
- Yoo S, Myszka DG, Yeh C-Y, McMurray M, Hill CP, Sundquist WI. 1997. Molecular recognition in the HIV-1 capsid/cyclophilin A complex. *J Mol Biol* 269:780–795.
- Zachariasen WH. 1947. Direct determination of stacking disorder in layer structures. *Phys Rev* 71:715–717.
- Zachariasen WH. 1948. Crystal chemical studies of the 5f-series of elements. III. A study of the disorder in the crystal structure of anhydrous uranyl fluoride. *Acta Crystallogr* 1:277–281.
- Zhao Y, Chen Y, Schutkowski M, Fischer G, Ke H. 1997. Cyclophilin A complexed with a fragment of HIV-1 gag protein: Insights into HIV-1 infectious activity. *Structure* 5:139–146.
- Zhao Y, Ke H. 1996. Crystal structure implies that cyclophilin predominantly catalyzes the *trans* to *cis* isomerization. *Biochemistry* 35:7356–7361.